Detection of Nematodes in Cod (*Gadus morhua*) Fillets by Imaging Spectroscopy

KARSTEN HEIA, AGNAR H. SIVERTSEN, SVEIN K. STORMO, EDEL ELVEVOLL, JENS PETTER WOLD, AND HEIDI NILSEN

ABSTRACT: A promising method for detection of parasites in whitefish fillets has been developed. By use of imaging spectroscopy it is possible to record both spectral and spatial information from an object. In this work it is shown that by applying a white light transmission setup and imaging spectroscopy to cod (*Gadus morhua*) fillets, it is possible to make spectral images containing information to differentiate between fish muscle and parasites. The spectral images are analyzed by discriminant partial least square regression as well as image-filtering techniques. The method identifies parasites on the surface of the fillets as well as embedded parasites. One parasite was detected at 0.8 cm below the fillet surface, which is 2 to 3 mm deeper than what can be found by manual inspection of fish fillets. The method is nonintrusive and should thus be feasible for industrial purposes.

Keywords: fish, imaging spectroscopy, instrumental detection, multivariate analysis, parasites

Introduction

Presence of parasites, also known as nematodes or roundworms, in whitefish is a naturally occurring phenomenon. In Atlantic cod (*Gadus morhua*) the most abundant parasites found are *Pseudoterranova decipiens* and *Anisakis simplex*. The parasites undergo several egg and larval stages during their life cycle, and the different stages require different host organisms for growth and development (Hafsteinsson and Rizvi 1987; McClelland 2002). *A. simplex* is more abundant in offshore fish, whereas *P. decipiens* is more likely to be found in inshore fish (Marcogliese 2002).

Human consumption of parasites in fish muscle is generally not considered a health issue as long as the fish is exposed to normal cooking temperature or freezing. By cooking or freezing the parasites are killed and are thus no longer regarded as a health risk. European Community regulations on fish and fish products for human consumption demand that species intended for marinating or salting at temperatures below 60 °C must be stored at −20 °C for a minimum of 24 h. The requirements of the U.S. Food and Drug Administration are even stricter, demanding storage for −23 °C for a period of 7 d (Audicana and others 2002). Consumption of infected material from raw or marinated fish or also undercooked parts of the fish can cause clinical signs of anisakiasis. These signs may include nausea, abdominal discomfort, or vomiting (Margolis 1977; McClelland 2002); however, in a recent review by Audicana and others (2002) it was questioned whether temperature treatment is sufficient to eliminate the health risk upon consumption of parasite-infected fish material.

Nematode infection may be a frequent problem, but it is not well known to the majority of fish consumers. In general, the finding of parasites in fish muscle will cause immediate consumer rejection of the product, and it might also lead to distrust of fish as a healthy and wholesome product. It is known that media exposure of the problem has led to significant reduction of fish consumption (Fischler 2002). Such incidences clearly state how easily consumer trust is shattered, and hence fish processors are willing to invest both money and labor to avoid the presence of parasites in fish products.

At present the commercial way of detecting parasites is by means of candling and manual inspection. The fillets are placed onto a white light table, and parasites embedded to a depth of 6 mm into the fillet can be spotted and removed manually; however, the detection efficiency is reported to be low; an average of only 60% to 70% (Bublitz and Choudhury 1992) of the parasites are detected and removed, and hence a number of parasites are left in the muscle and potentially found by the unlucky consumer.

During the past few decades a number of different techniques have been explored as possible instrumental methods for parasite detection in whitefish. In 1970, Pippy suggested the use of fluorescence to spot parasites. The company Lumetech (Hellerup, Denmark) included this method as part of their processing equipment in the early 1990s; however, the method was limited to the detection of surface nematodes as the ultraviolet light does not penetrate deeply into the fish muscle. To our knowledge the fluorescent detection method is no longer commercially available. Hafsteinsson and others (1987, 1989) reported detection of parasites deeply embedded into the fish muscle by use of ultrasonic waves. The parasite is differentiated from the fish tissue by a difference in acoustic properties. One problem of the ultrasonic method is the requirement of direct coupling between detector and measurement medium, and this is one reason why the technique has not been industrialized. Jenks and others (1996) obtained promising results by measurement of the electrical conductivity in fish and parasites. The method, however, requires the fillet to be placed in a saline solution and this may be impractical in view of possible industrialization.

A thorough study of the optical properties of fish muscle and nematodes was given by Petursson (1991). In this work the issues of light absorption and the significant scattering of light in fish tissue were described. Detection by candling is based on human vision and the ability to register differences in color and structure. An instrumental detection method based on the optical properties of the fish muscle and the parasites is therefore considered of interest. In a work by Stormo and others (2004) it was shown that both *P. decipiens* and

MS 20060338 Submitted 6/15/2006, Accepted 10/9/2006. *Authors Heia, Sivertsen, and Nilsen are with Fiskeriforskning, N-9291 Tromsø, Norway. Authors Stormo and Elvevoll are with Norwegian College of Fishery Science, Univ. of Tromsø, N-9037 Tromsø, Norway. Author Wold is with Matforsk, Osloveien 1, N-1430 Ås, Norway. Direct inquiries to author Nilsen (E-mail: heidi.nilsen@fiskeriforskning.no).*

doi: 10.1111/j.1750-3841.2006.00212.x

A. simplex contain substances absorbing light in the ultraviolet and lower visible light range, whereas cod muscle did not. Multispectral images coupled with multivariate analysis techniques have proven useful for parasite detection in whitefish fillets (Wold and others 2001). This technique is promising in view of speed and the non-intrusive approach. Spectral imaging is a relatively recent method (Herrala and Okkonen 1996; Hyvarinen and others 1998; Sigernes and others 1998, 2000) resembling human vision with respect to simultaneous registration of light absorption and scattering as well as spatial effects of an object.

The objective of this work was to investigate the ability of detecting parasites by means of imaging spectroscopy and multivariate analysis techniques. It is also of interest to identify which wavelength ranges are important when differentiating between fish muscle and parasites. These findings will be of importance for developing instrumental systems for industrial automatic parasite detection.

Material and Methods

Cod

Eight cod (*Gadus morhua*), bled, deheaded, and gutted, were purchased from a local fish company located off Tromsø, Norway. The cod originated from a line catch in local waters. Gutted and deheaded weight varied from 1.5 to 2.4 kg. The fish were manually filleted and skinned prior to freezing. The fillets were frozen at −20 °C for 1 wk, and were then thawed at 5 °C previous to spectroscopic measurements. Upon manual inspection of the fillets, parasites were identified both on the fillet surface and embedded in the fish muscle. The parasite depth from the fillet surface was measured manually by use of a Vernier calliper. The nematodes were varying in color; dark and light brown as well as red ones were found, and they were mainly found in the characteristic curled shape. The length of the parasites varied between 2 and 4 cm. Spectroscopic measurements were performed on intact cod muscle with naturally embedded nematodes, and the fillet area measured was the loin and the belly flap.

After the imaging measurements were made the fillets were cut into 5 to 6 mm slices to identify parasites too deeply embedded to be found by visual inspection of the whole fillets. The fillets used for measurements also contained bloodspots and black lining.

Imaging spectrograph

To collect data with both spatial and spectral information the instrument SpexTubeIV (Sigernes and others 2000) was applied. SpexTubeIV uses a rotating mirror in front of the spectrograph in order to achieve full spatial resolution. For a fixed mirror position 1 line across the sample is imaged with full spectral information in the range from 350 to 950 nm. The principle of spectral imaging of an object can be described in 2 steps: First, light from the object must be focused by a lens or mirror to form an image at the spectrograph's entrance slit plane. The resulting spectrogram is the intensity distribution as a function of wavelength and position along the slit. The diffracted slit image contains both spectral and spatial information along a narrow track of the object. The spectrum was collected using 2 measurements with different grating angles, resulting in 2 partly overlapping wavelength regions: 350 to 610 nm and 530 to 950 nm. Spectral resolution of the system was approximately 2 to 3 nm.

Second, in order to obtain the object's full spatial extent, it was necessary to sample along the whole object. This required the use of a high-resolution rotary element. The idea was to record spectrograms for each track of the object as the image at the entrance plane was moved across the slit. A front surface mirror in front of the focusing element was used in combination with a high-resolution stepper motor. In fact, the use of a mirror enabled us to sample target objects that were static or moving relatively to the instrument by rotating or keeping the mirror fixed, respectively. The spatial resolution of the imaging system was 0.5 mm × 0.5 mm.

In short, 1 spectral image of a fillet sample contained 290 × 290 pixels, where each pixel was represented with a spectrum ranging from 350 to 950 nm. Figure 1 shows a sketch of the instrumental setup with a description of the different elements. In this case the light source was positioned below the fillet, hence a transmission measurement setup.

Data analysis

The tool used for data analysis was discriminant partial least square (DPLS) regression implemented in the software IDL (Interactive Data Language, 6.0, Research Systems Intl. Ltd, Berkshire, United Kingdom). The aim of the analysis was to evaluate the capability of identifying nematodes embedded in fish muscle based on spectral information. DPLS regression was made to combine and assess the spectral information in order to identify pixels representing fish sample with embedded nematodes.

For training, visual inspection of the fillets and the spectral images were used to select a subset of pixels with known class membership, nematode, or fish muscle. The X-matrix was constructed using the selected subset of pixels from the spectral images. Each row in the X-matrix consisted of the mean centered full spectrum from 1 pixel. The elements of the Y-vector used for training were designed with ones and zeros representing nematode and fish muscle, respectively.

For classification of new samples the trained DPLS model was applied on each pixel in the spectral image. The classifier output was numbers around one and zero representing nematode and not nematode, respectively. Hence the multispectral image was reduced to a single-band image representing the classification result.

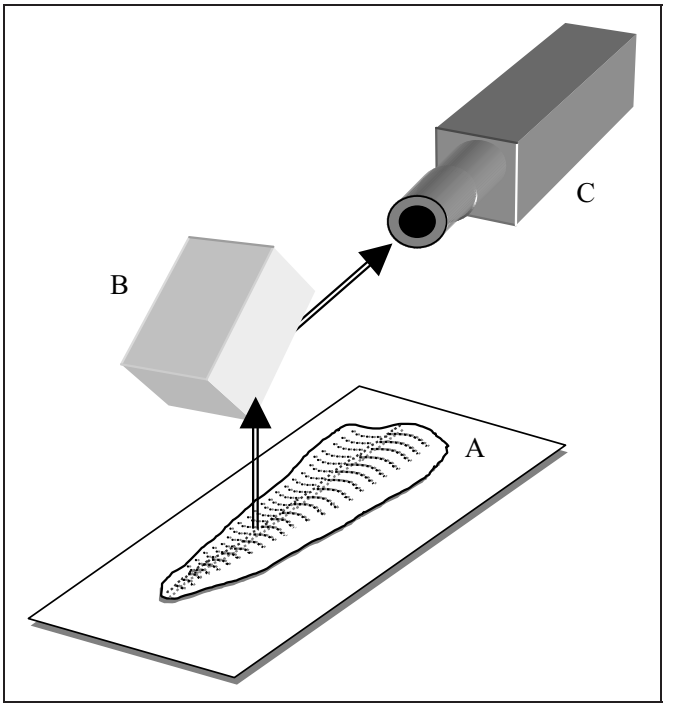

Figure 1—The experimental setup used to collect imaging spectroscopy data. The light source was positioned below the sample (A). The light passed through the sample (A), and was then reflected by the mirror (B) before it entered the spectrograph (C) through an entrance slit. Spatial resolution along the fillet was obtained by rotating the mirror between exposures.

Image processing

Image analysis was made by selecting different threshold values to identify parasite data from the DPLS classification result. The threshold value decided how well the classifier performed: too high a value would mean that not all nematodes would be detected while too low a value would introduce false positives. The solution was to select a threshold value that ensured that the nematodes were detected with a minimum number of false positives.

The number of false positives, in terms of impulse noise, can be reduced by applying a median filter (Gonzales and Woods 1992) on the thresholded DPLS classification image. The size of the median filter must be selected in a way so that the correctly detected nematodes are not removed from the result of the analysis.

Results and Discussion

Five parasite-infected cod fillets were measured using the SpexTubeIV instrumentation, covering the wavelength range from 350 to 950 nm. Training data were collected from three of the fillets, covering nematodes of different color as well as placement and location in the fillets. Black lining and blood spots in the muscle and fish muscle without any recognizable defects were also present in the measured data. Based on the training data a DPLS model with 9 components was built and applied on the collected spectral images for classification. Figure 2 shows the regression plot for this model, where some wavelength bands for identification of nematodes are indicated. Upon visual inspection of the plot the wavelength bands are centered on 440, 480, 510, 550, 570, 580, 600, and 680 nm. The bands in the range around 500 nm may be due to the absorption characteristics of blood (Wold and others 2001). Identifying the wavelengths that give the best discrimination between parasites and fish muscle is of interest both for analytical purposes and for designing a cost-efficient instrument for automated parasite detection.

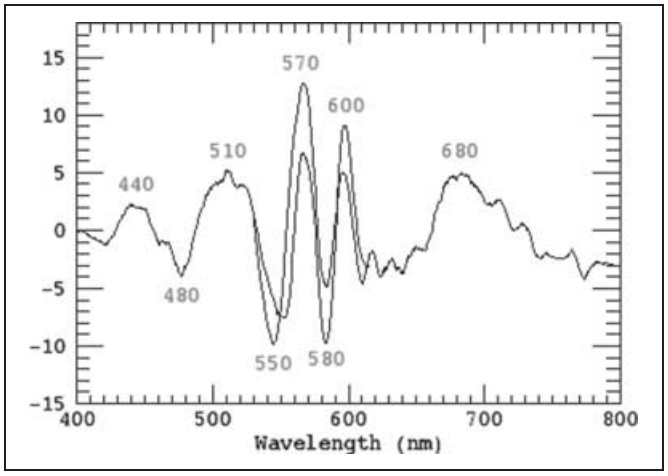

Figure 2—Regression plot for the DPLS model developed for nematode detection. Important wavelength regions for nematode detection were denoted with wavelength information. The overlapping spectral curve in the region 530 to 610 nm was due to the system characteristics. This spectral region was recorded with 2 different grating angles.

The model made from three of the spectroscopic recordings was applied on the remaining measurement data. Example results are given in Figure 3 to 6. Figure 3(a) shows an image of the sample captured with a standard digital camera. In Figure 3(b) the image plane, from SpexTubeIV, representing 540 nm is shown with marked nematodes, blood spots, and black lining. The result from applying the DPLS regression is shown in Figure 3(c) where the classification before applying the threshold is positioned in green on top of the original image. As can be seen from this figure some nematodes are clearly visible while those deeply embedded appear more diffuse. The 5 nematodes marked in Figure 3(b) were different in color and were located at different fillet depths; see Table 1.

Thresholding the output from the DPLS classification at different levels shows that this is a crucial step for identifying the parasites; see Figure 4. Using a threshold level larger than 0.3 only 2 of 5 nematodes are recognized as nematodes. Applying a threshold level at 0.3 the 3rd nematode is visible, while all 5 nematodes are detected when the threshold is 0.2. At this low threshold level there were also several false positives as can be seen in Figure 4(d).

To clean up the classification results for false positives a median filter can be applied to the output from the previous step. Figure 5 shows 4 different approaches with median filters applied on the image data. Most of the impulse noise in the classification was removed after 1 run with a median filter, Figure 5(a) and (c), with a filter size of 3×3 and 5×5, respectively. After a 2nd run with the same filter size, Figure 5 (b) and (d), all impulse noise was removed. The size of the median filter may also affect the final result of detection as can also be seen from Figure 5. Comparing Figure 5 (a) and (c) shows that a filter size of 5×5 was almost removing nematode K1 from the classification result, while a 3×3 median filter was not doing that. Even after a 2nd run with a 3×3 median filter nematode K1 was still present. With a filter size of 5×5 a 2nd run removed this nematode completely.

Fixing the parameters in the classification procedure to a threshold level of 0.2 followed by 2 runs with a 3×3 median filter, the DPLS regression was tested on the data set. Figure 6 gives examples of the analytical result of these settings. The 4 fillet samples in Figure 6 were identified to contain 16 parasites; see Table 2. Comparing the analytical findings with the result of manual inspection of sliced samples showed that all nematodes were detected by imaging spectroscopy. One of the instrumentally found parasites was

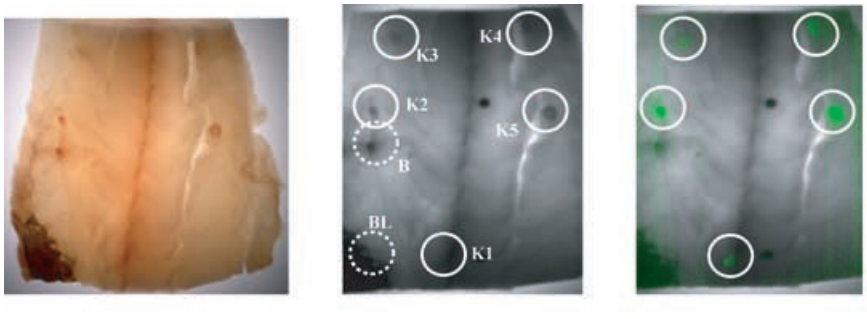

Figure 3—Section of cod fillet. (a) Image of the cod sample captured with digital camera. (b) Imaging spectroscopy image at 540 nm where the nematodes, K1 to K5, are indicated with white circles, a blood spot, B, marked with a dotted circle and black lining, BL, marked with a dotted circle. (c) Classification result, in green, on top of the 540 nm image before thresholding. To the eye the bloodspot may appear as a parasite. Bloodspots were not identified as parasites by the classification.

embedded 8 mm into the fish fillet, and detection at this depth is beyond the detection limit of manual inspection by means of candling. This deeply embedded parasite was found by slicing the fillet and could not be seen upon visual inspection of the intact fillet. The analysis performed with this setting, however, also resulted in some false positives as seen in Figure 6. The more sensitive the algorithm is in terms of finding parasites, the more likely it is to introduce false positives in the classification result. Also, due to light scattering effects in the fish muscle, the analytical identification of parasites in data sets does not necessarily correspond to the physical size of the parasites. Examples of this are seen on the identification of parasites p10 and p11. Here the analysis indicates very large parasites present, but the actual parasites did not differ from the others.

From the viewpoint of the fish-processing industry the main focus of nematode detection should be those parasites that can be seen by the consumer. In that perspective the efficiency of the classification procedure can be reduced, allowing deeply embedded nematodes to pass without detection. This will be the case if the threshold value increases and this will also significantly reduce the number of false positives.

The above-described procedure of analysis also enabled detection of parasites embedded as deep as 0.8 cm into the fish fillet. This finding is deeper into the fish muscle than what is considered possible to find by means of manual inspection. In this respect these results are very promising, indicating that instrumental detection may perform better than today's manual procedure. Imaging spectroscopy as shown here and the multispectral image approach as shown by Wold and others (2001) are also feasible in view of the on-line requirements of the fish-processing industry. This optical approach may thus represent a long-sought solution to the problem of automated parasite detection for the fish-processing industry.

Table 1 — Depth and color information for the 5 nematodes marked in Figure 3(b)

Parasite nr	Depth into the fillet (mm)	Color
K1	3	Light red/white
K2	1	Red
K3	5	Light red/white
K4	2	Red
K5	1	Red

Conclusions

Methodology for instrumental and automated parasite detection in fish fillets has long been a scientific issue. The findings of this work demonstrate the potential of imaging spectroscopy as a tool for instrumental parasite detection in whitefish fillets. The method proves to identify parasites located from the fillet surface and embedded into the fillet as deep as 0.8 cm. This enables detection deeper into the fillet than what is considered possible by means of manual inspection. Further development and

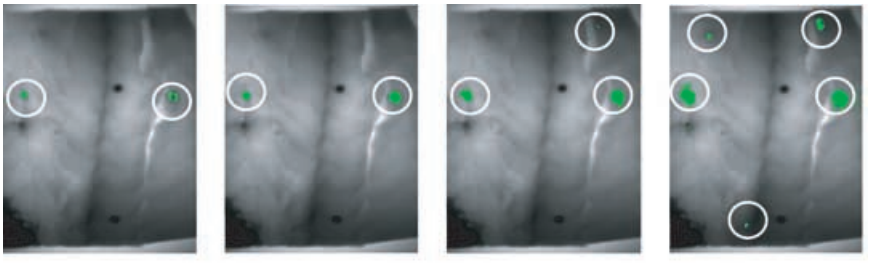

Figure 4 — Same section of cod fillet as shown in Figure 3. The classification result after thresholding. White circles indicate which parasites were detected. The thresholded classification, denoted with green color, is put on top of the 540 nm image. (a) – (d). Threshold levels set at 0.7, 0.5, 0.3, and 0.2 in images a, b, c, and d, respectively.

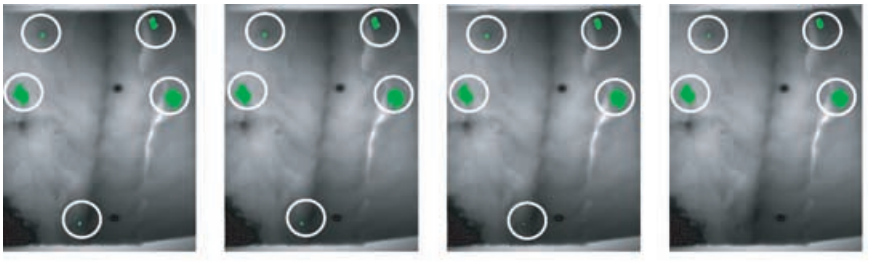

Figure 5 — Same section of cod fillet as in Figure 3 and 4. Median filtered classification results, threshold level 0.2. (a) and (b): 3 × 3 median filter applied once and twice, respectively. (c) and (d): 5 × 5 median filter applied once and twice, respectively. White circles indicate which parasites were detected.

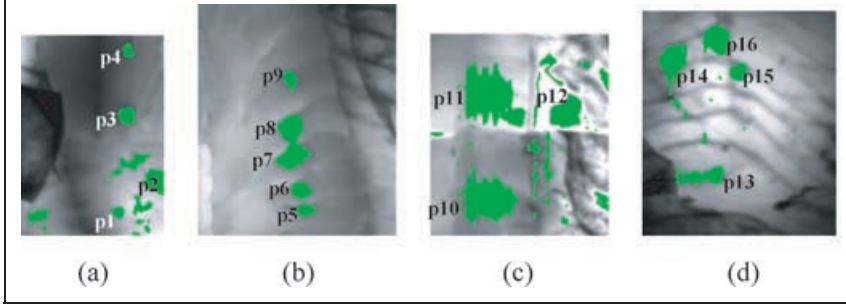

Figure 6 — Example classification results of parasites in cod fillets. The threshold level was fixed at 0.2 followed by 2 runs with a 3 × 3 median filter. Green spots, p1 through p13, indicate findings of parasites. How deep the parasites were embedded into the fillets is shown in Table 2. (a) Loin and belly flap with black lining, sample thickness 5 to 12 mm; (b) loin, sample thickness 20 to 25 mm; (c) loin and belly flap with black lining, sample thickness 5 to 20 mm; (d) belly flap, sample thickness 7 to 10 mm.

Table 2—Registered depth of parasites found in fillets imaged in Figure 6. The parasites may be curved in the fillet in such a way that the depth into the fillet is a given range rather than fixed depth.

Parasite nr	Depth into the fillet (mm)
p1	1–2
p2	3
p3	5
p4	2–3
p5	3
p6	3
p7	3
p8	5
p9	8
p10	3–4
p11	4–6
p12	0–1
p13	1
p14	3
p15	2–3
p16	3–5

optimization on the instrumental technology as well as the analytical tools is, however, required to make this method commercially viable.

Acknowledgment

This project was funded by Norwegian Research Council and the Fishery and Aquaculture Industry Research Fund in Norway.

References

Audicana MT, Ansotegui IJ, de Corres LF, Kennedy MW. 2002. *Anisakis simplex*: dangerous—dead and alive? Trends Parasitol 18(1):20–5.

Bublitz CG, Choudhury GS. 1992. Effect of light intensity and color on worker productivity and parasite detection efficiency during candling of cod fillets. J Aquat Food Prod Technol 1(2):75–88.

Herrala E, Okkonen J. 1996. Imaging spectrograph and camera solutions for industrial applications. Intern J Pattern Recognit Artif Intell 10:43–54.

Hyvarinen TS, Herrala E, Dall'Ava A. 1998. Direct sight imaging spectrograph: a unique add-in component brings spectral imaging to industrial applications. In: Williams GM Jr,. editor. Digital solid state cameras: designs and applications, Proc SPIE 3302:165–75.

Jenks WG, Bublitz CG, Choudhury GS, Ma YP, Wikswo JP. 1996. Detection of parasites in fish by superconducting quantum interference device magnetometry. J Food Sci 61(5):865–9.

Fischler C. 2002. Food selection and risk perception. In: Anderson GH, Blundell J, Chiva M, editors. Proceedings from the symposium Food selection, from genes to culture. Paris, France: Danone Inst., p 135–51.

Gonzales RC, Woods RE. 1992. Digital image processing. Boston, Mass.: Addison-Wesley Publishing Co. p 716.

Hafsteinsson H, Rizvi SSH. 1987. A review of the sealworm problem: biology, implications and solutions. J Food Prot 50(1):70–84.

Hafsteinsson H, Parker K, Chivers R, Rizvi SSH. 1989. Application of ultrasonic waves to detect sealworms in fish tissue. J Food Sci 54(2):244–7, 273.

Marcogliese DJ. 2002. Food webs and the transmission of parasites to marine fish. Parasitology 124:83–99.

Margolis L. 1997. Public health aspects of "codworm" infection: a review. Fish Res Board Canada 34(7):887–98.

McClelland G. 2002. The trouble with sealworms (*Pseudoterranova decipiens* species complex, Nematoda): a review. Parasitology 124:183–203.

Petursson J. 1991. Optical spectra of fish flesh and quality defects. In: Pau LF, Olafsson R, editors. Fish quality control by computer vision. New York: Marcel Dekker, Chap. 3, p 45.

Pippy JHC. 1970. Use of ultraviolet light to find parasitic nematodes in situ. J Fish Res Bd Canada 27:963–5.

Sigernes F, Heia K, Nilsen H, Svenøe T. 1998. Imaging spectroscopy applied in the fish industry? Norw Soc Image Process Pattern Recogn 2:16–24.

Sigernes F, Lorentzen DA, Heia K, Svenøe T. 2000. Multipurpose spectral imager. Appl Opt 39(18):3143–53.

Stormo SK, Ernstsen A, Nilsen H, Heia K, Sivertsen AH, Elvevoll E. 2004. Compounds of parasitic roundworm absorbing in the visible region: target molecules for detection of roundworm in Atlantic cod. J Food Prot 67(7):1522–5.

Wold JP, Westad F, Heia K. 2001. Detection of parasites in cod fillets by using SIMCA classification in multispectral images in the visible and NIR region. Appl Spectrosc 55(8):1025–34.